




Extremely narrow sharply peaked resonances at the edge of the continuumIgnas Lukosiunas ^{1,*}, Lina Grineviciute,² Julianija Nikitina ², Darius Gailevicius ¹ and Kestutis Staliunas ^{1,3}¹*Vilnius University, Faculty of Physics, Laser Research Center, Sauletekio Avenue 10 LT-10223, Vilnius, Lithuania*²*Center for Physical Sciences and Technology, Savanoriu Avenue 231, LT-02300 Vilnius, Lithuania*³*ICREA, Passeig Lluís Companys 23, 08010, Barcelona, Spain
and UPC, Departamento de Física, Rambla Sant Nebridi 22, 08222, Terrassa (Barcelona), Spain*

(Received 18 October 2022; accepted 9 May 2023; published 8 June 2023)

We report a critical narrowing and sharpening of resonances of a potential well when their eigenfrequencies approach the edge of the continuum. The resonances also obtain sharply peaked shapes with the discontinuity of their slopes. The situation can be realized for an electromagnetic wave propagating across dielectric thin films with a periodically modulated interface(s). We show the phenomenon semianalytically on a general model of a driven quantum potential well, and also by rigorous numerical analysis of Maxwell equations for the wave propagation across the thin film with a modulated interface(s). We justify the phenomenon experimentally, by measurements of light reflection from a dielectric thin film deposited on a periodically modulated surface. The narrow and sharply peaked resonances can be used for an efficient narrow-band frequency and spatial filtering of light.

DOI: [10.1103/PhysRevA.107.L061501](https://doi.org/10.1103/PhysRevA.107.L061501)**I. INTRODUCTION**

It is well known that the wave functions in a potential well can form bound states for their energies below the background of the potential well, and the continuum states for their energies above the background. Although basic wave behavior in the potential wells has been established since the beginning of quantum mechanics [1], new findings are constantly being reported. One such example is the phenomenon of bound states in the continuum, recently proposed for the potentials of a special form [2,3]. Here we report critical narrowing of the resonances and extreme sharpening of the peaks of the resonances when their energies approach the background energy of the potential well, just before crossing the boundary of the continuum.

The resonances of the discrete states follow the universal Lorentzian shapes when the energies are deep in the potential well. What happens when the potential is continuously deformed so that the energy of one of its discrete states crosses the edge of the continuum (EOC), as illustrated in Fig. 1? This Letter shows that the width of the resonances strongly decreases, and the resonances obtain sharply peaked shapes at the crossing point. Moreover, the scaling of the resonance width with the coupling constant also becomes unusual: whereas the width of the Lorentz resonance scales as the power of 2 with the coupling constant, the width of the resonance at the EOC scales as a power of 4. In this way, the resonances with special properties are reported, which on the one hand, are intriguing mathematical-physical objects, and on the other hand, have a practical application potential. The

effect might be useful to realize extremely narrow-band and sharp-contrast frequency and angular (spatial) filters.

In this Letter we mathematically relate the problem of electromagnetic wave diffraction on interface-modulated thin dielectric films with the problem of a particle's wave function in a driven potential well, Fig. 1. The wave propagation across such thin films has been previously studied, mostly numerically, by the rigorous coupled wave approach, in the context of its angle-wavelength transmission peculiarities [4–12], or Fano-like resonances [13–15]. The analogy between the thin films and the driven potential well, explored in the present work, allows us to calculate the energy states in the potential well, corresponding to the thin film planar modes, and to explore these resonances semianalytically. We calculate the asymptotic shapes and estimate the scaling of the width of the resonances in a simplified model system of a driven potential well. We apply rigorous numerical methods to calculate the light reflection or transmission through the modulated thin films and identify these narrow resonances in reflection angle-wavelength spectra. Finally, we fabricate a structure by physical vapor deposition (PVD) on a corrugated surface and measure the predicted narrow-band sharp resonances in the reflection angle-wavelength spectra.

II. SIMPLIFIED MODEL

In analytical treatment, we separate the electromagnetic radiation into the near-to-normal part (corresponding to the incident, reflected, and transmitted modes) and the guided radiation part (parallel to the film surface). Specifically, we define the near-to-normal wave as $A_0(x, z, t) = A_0(z)\exp(ik_{0,z}z + ik_{0,x}x - i\omega t)$, where $k_{0,x}^2 + k_{0,z}^2 = k_0^2 = \omega^2/c^2$, which can be considered as the Fabry-Perot (FP) mode of the resonator formed by a thin film of

*Corresponding author: ignas.lukosiunas@ff.vu.lt

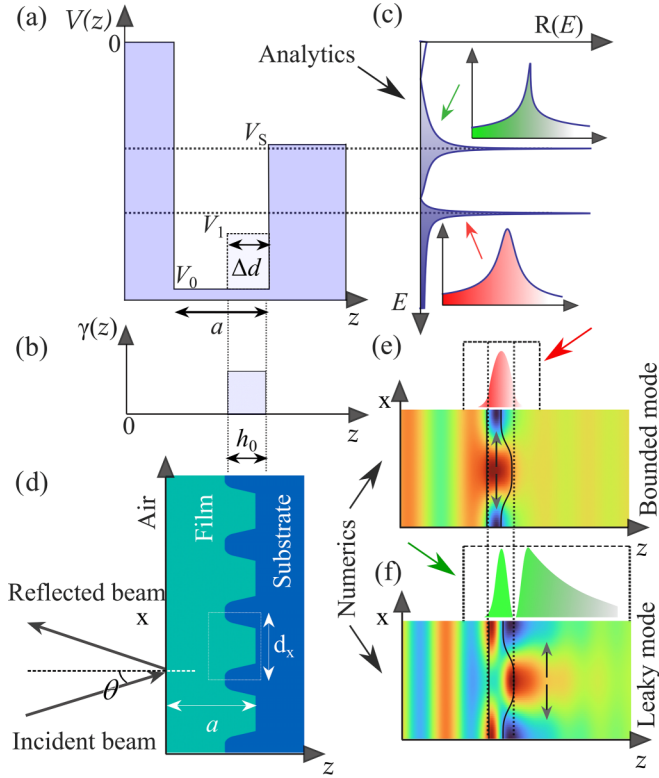


FIG. 1. Driven potential well (a,b) is equivalent to the film of high refractive index with periodically modulated interface (d). The interface modulation couples the nearly normal FP mode into the bounded waveguided modes (e) or broadened leaky surface modes (f), resulting in usual Lorentz or sharply peaked resonances, respectively (c). The modification of the refraction index in the coupling area is shown by the line in (a).

a refraction index higher than that of the surrounding material. We also define the guided radiation as $A_1(x, z, t) = A_1(z)\exp(ik_{1,x}x - i\omega t)$. Note that the shapes of both radiation components depend solely on the coordinate z . The near-normal and guided components are mutually coupled due to the periodic modulation of the thin film interface, with the period d_x of the order of the wavelength of the incident wave: $k_{1,x} = k_{0,x} \pm q$. For analytical treatment we consider only the first diffraction order: $q = 2\pi/d_x$, and also only one diffracted mode, for instance, the one with $k_{1,x} = k_{0,x} + q$. Then the stationary wave equation for the guided radiation component $A_1(z)$ reads

$$\frac{\partial^2 A_1(z)}{\partial z^2} + \left[\frac{\varepsilon(z)\omega^2}{c^2} - (k_{0,x} + q)^2 \right] A_1 = 0. \quad (1)$$

Equation (1) is rigorous for the case of s -polarized waves, when the electric field oscillates along the modulation grooves, i.e., along the coordinate y (the p -polarized waves also allow a semianalytical treatment (see Sec. B in the Supplemental Material [16]), resulting in the same qualitative physical picture). Equation (1) is identical to the stationary Schrödinger equation for the quantum particle with the energy $E = k_0^2 - (k_{0,x} + q)^2$ in the potential well with the profile $V(z) = [1 - \varepsilon(z)]k_0^2$ as illustrated in Fig. 1(a). Such a potential supports the bound states, which correspond to the planar

modes of the thin film. Coupling between the FP radiation $A_0(z)$ to these planar modes $A_1(z)$ results in the Fano-type resonances, studied, for instance, in [13–15]. We introduce the coupling between FP radiation and the guided radiation by additional external driving for the latter component:

$$\frac{\partial^2 A_1(z)}{\partial z^2} + [E - V(z)]A_1(z) - i\gamma(z)e^{ik_{0,z}z}A_0(z) = 0. \quad (2)$$

$\gamma(z)$ is the normalized coupling profile along z ; see Fig. 1(b). For analytical treatment, we consider the uniform coupling over the area in z of thickness h_0 , $\gamma(z) = \gamma_0/h_0$, γ_0 being a dimensionless net coupling coefficient, and $\gamma(z) = 0$ elsewhere. The estimation of γ_0 in the limit of a shallow harmonic modulation of the interfaces has been provided, for instance, in [13]: $\gamma_0 \approx h_0 \Delta n / \lambda$, where h_0 is the amplitude of the surface modulation of the film: $h(x) = h_0/2\cos(qx)$, and Δn is the difference in the refractive indices of materials forming the modulated interface. To maximally fit the quantum-potential-based model to the experiment we also modify the potential $V(z)$ by deforming its bottom on the interaction section: $V_1 = fV_0 + (1-f)V_s$, i.e., considering the f -weighted average of the bottom and right-background potentials, V_0 and V_s . The presence of a step, indicated by the line in Fig. 1(a), is not essential to the main results.

Equation (2) can be solved by finding piecewise the wave function in each sector of the potential, s , along z : $A_{1,s}(z) = a_{0,s}e^{ik_{0,z}z} + a_{+,s}e^{ik_{z,s}z} + a_{-,s}e^{-ik_{z,s}z}$ with $k_{z,s}^2 = (E - V_s)$, $a_{0,s} = i\gamma_s A_{0,s} / (E - V_s - k_0^2)$, and matching the solutions and their derivatives on the interfaces between the sectors to determine the $a_{+,s}$ and $a_{-,s}$. The solutions were obtained in an explicit analytical form for the driven potential shown in Fig. 1; however, they are not analytically tractable due to their algebraic complexity.

To calculate the transmission/reflection of the incident field through the film, it is convenient to introduce the gain of the FP mode (see Sec. C in the Supplemental Material [16]):

$$g_0 = \frac{i}{A_0} \int \gamma(z)A_1(z)e^{-ik_{0,z}z} dz. \quad (3)$$

The physical sense of gain g_0 is the feedback from the guided modes back to the FP mode. The transmission and reflection of the incident wave through the thin film then read: $t_{\text{FP}} = (1 - g_0/t^2)^{-1}$, $r_{\text{FP}} = g_0/t^2(1 - g_0/t^2)^{-1}$. (We consider that the transmission coefficient through the interfaces, t , is equal for both interfaces.) The reflection and transmission of the incident radiation obeys the relation $T + R = |t_{\text{FP}}|^2 + |r_{\text{FP}}|^2 = 1$.

The analysis model above identifies the Fano-type resonances [17], with the asymptotical (at their peak) parabolic shapes. We varied the depth of the potential well V_0 to tune the frequencies of the resonances to explore the crossing of the highest energy resonance through the EOC. The width of the resonance remains nearly constant for its frequency deep in the potential well but starts decreasing when approaching the EOC. Meanwhile, the maximum value of the reflection coefficient remains unity. The top reflection coefficient decreases after crossing the continuum boundary, as indicated in Fig. 2(a). The shape of the resonance curve becomes sharply peaked at the EOC, as expected.

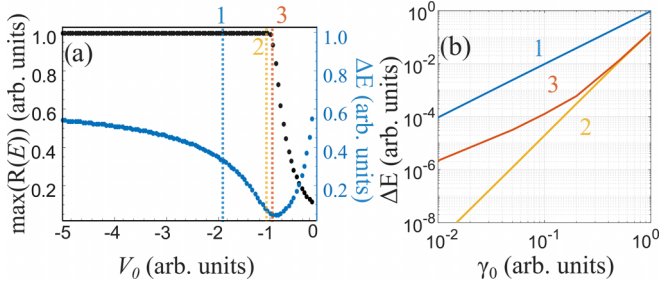


FIG. 2. (a) The maximum of reflection coefficient from the potential well, $\max[R(E)]$, and the half-width of the reflection resonance ΔE_0 depending on V_0 . $\gamma_0 = 0.75$. (b) The half-width of the reflection resonance ΔE_0 depending on the coupling constant γ_0 at the EOC: $V_0 = -1$, yellow line, slightly below the EOC; $V_0 = -1.05$, red line, and deep below the EOC; $V_0 = -2$, blue line. Other parameters are $a = \pi/2$, $h_0 = \pi/10$.

III. RESONANCES

The potential well in Fig. 1 did not lead to simple algebraic expressions. To maximally simplify the problem and to get analytic estimations, we further simplified the model. We considered a semi-infinite potential well, with $V \rightarrow \infty$ for $z < 0$, and constant driving force throughout the entire bottom of the potential well $0 < z < h_0$. The analysis (see Sec. C in the Supplemental Material [16]) leads to the tractable expressions of the gain function in a limiting case of the narrow and deep potential well ($ak_{0,z} \ll 1$, $|V_0| \gg 1$):

$$g_0 = \frac{\gamma_0^2 i\sqrt{V_0} 2k_2^2 + (k_1^2 - 2k_2^2)\cos(ak_1)}{a^2 k_1^3 k_2 \cos(ak_1 + \phi)}. \quad (4)$$

Here $\tan(\phi) = ik_2/k_1$, $k_1 = \sqrt{E - V_0}$, and $k_2 = \sqrt{E}$ are the wave numbers of the wave function in the potential well and outside the well, respectively. For the bounded states $E < 0$ the k_2 is imaginary valued, whereas k_1 remains real valued.

The poles of (4), $\cos(ak_1 + \phi) \rightarrow 0$, indicate the resonances, which occur for $(ak_1 + \phi) \rightarrow \pi(2n + 1)/2$, where the integer n counts the resonances starting from $n = 0$. We simplify (4) in two different asymptotics:

(1) The lowest energy-bound state lies deep in the potential well, $E, V_0 \rightarrow -\infty$. Then $|k_1| \ll |k_2|$, $\phi \rightarrow -\pi/2$, $\cos(ak_1 + \phi) \rightarrow 0$, $ak_1 \rightarrow \pi$ (for the lowest energy bound state):

$$g_0 = \frac{2i\gamma_0^2}{a^2} \frac{1}{\sqrt{a^2 - \pi^2/V_0}} \frac{1}{\Delta E}. \quad (5)$$

In the limit $V_0 \rightarrow -\infty$, the half-width of the gain line simplifies to $\Delta E_0 = 2\gamma_0^2/a^3$, and scales with the coupling coefficient as $\Delta E_0 \sim \gamma_0^2$. This case corresponds to the Fano-like resonances of the discrete states.

(2) The lowest energy-bound state coincides with the background level on the right side of the potential well at $z > a$, $E = 0$. Then $|k_2| \ll |k_1|$, $\phi \rightarrow 0$, $\cos(ak_1) \rightarrow 0$, $ak_1 \rightarrow \pi/2$, and we obtain

$$g_0 = \frac{-8\gamma_0^2}{\pi a^2} \frac{1}{\sqrt{\Delta E}}. \quad (6)$$

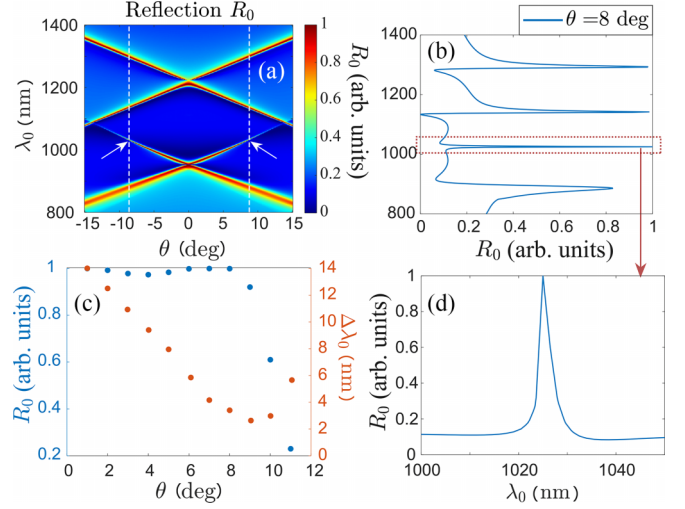


FIG. 3. The map of the reflection coefficient in the plane of angle wavelength (θ, λ) (a), and its cross section at a given angle θ (b). The arrows indicate the points corresponding to the resonance at the EOC. The top reflection coefficient and the resonance width of the highest frequency (smallest wavelength mode), depending on θ (c). The zoom of the reflection profile around the continuum edge (d). The calculations were performed by RCWA with the following parameters: modulation depth $h_0 = 200$ nm, modulation period $d_x = 625$ nm, layer thickness $d_z = 460$ nm, refraction indices $n_{\text{film}} = 2.25$, $n_{\text{substr.}} = 1.5$.

The half-width of the gain line becomes $\Delta E_0 = 64\gamma_0^4/(\pi^2 a^4)$, and scales with the coupling coefficient as $\Delta E_0 \sim \gamma_0^4$.

Equation (6) is the main result of our analytical study. For the positive detuning, $\Delta E > 0$, i.e., within the continuum, the gain is real valued, whereas for negative detuning, $\Delta E < 0$, i.e., below the EOC, the gain is imaginary. This has consequences for the reflection coefficient. For both positive and negative ΔE , the reflection coefficient asymptotically decreases as $R_{\text{FP}} \approx 1 - |\Delta E|/\Delta E_R$, with $\Delta E_R = 64\gamma_0^4/(\pi^2 t^4 a^4)$, which results in a sharply peaked shape of the resonance.

These analytic predictions were checked by numerically calculating the driven potential model, shown in Fig. 1. The sharply peaked resonances at the edge of the continuum were identified. The calculated width of the resonances (Fig. 2) indeed shows the predicted scaling. We recover the standard scaling of Lorenz resonances $\Delta E_0 \sim \gamma_0^2$ for the energies deep below the EOC and justify the $\Delta E_0 \sim \gamma_0^4$ scaling at the EOC.

IV. FULL MODEL

To prove the validity of the results obtained on simplified models, we performed the analysis using the rigorous coupled wave analysis (RCWA) [18,19]. Our own solver was developed for that purpose [16]. The results are summarized in Fig. 3.

The full model accounts for both (right or left propagating) guided modes. Therefore in Fig. 3 the pattern of the left- and right-inclined resonances in the parameter space of the incidence angle, and the wavelength (θ, λ), are

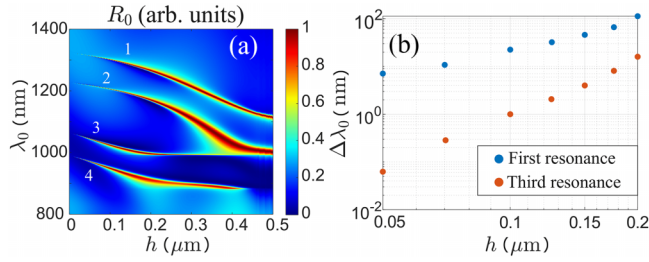


FIG. 4. (a) The map of the reflection coefficient in the plane of modulation depth versus wavelength. The width of the resonances versus modulation depth is shown in (b). The parameters are the same as in Fig. 3.

observed. The physical parameter space of the thin film (θ, λ) relates with the parameter space of the potential (V_0, E) via the above-presented relations: $E = k_0^2 - [k_0 \sin(\theta) + q]^2$, $V_0 = (1 - \varepsilon_{\text{film}})k_0^2$. The EOC corresponds to a particular set of parameters in (V_0, E), and equivalently in (θ, λ_0). These points are indicated in Fig. 3(a) by arrows for left- and right-guided waves. The inset shows the sharply peaked asymmetric resonance by crossing the EOC point along a particular $\theta = \text{const}$.

Resonance lines with only the smallest wavelength cross the EOC in Fig. 3. The other resonances, with the larger wavelength (lower energies), remain deep in the potential well. Consequently, their resonances do not develop sharp peaks, and remain Lorentzian, as Fig. 3(b) indicates.

The dependence of the top reflection coefficient and the resonance's width on the angle is shown in Fig. 3(c), in accordance with the conclusions from the simplified treatment above.

Finally, the scaling laws of the resonance width with the coupling coefficient (depth of the film interface modulation) were checked. If the usual Lorentz resonances show the well-established power 2 law, the resonances at the edge follow the power 4 law, as shown in Fig. 4(b).

V. EXPERIMENTAL REALIZATION

For fabricating such a structure, we used a commercially available fused silica surface grating (modulation period 625 nm, modulation depth 220 nm) with a nearly sinusoidal surface [see Figs. 5(a) and 5(b)]. The grating was used as a substrate for thin film deposition by PVD [20]. The ion beam sputtering technology [21] was used for Nb_2O_5 layer fabrication (thickness = 530 nm, refractive index 2.23); see also [22] for technological details. The profile of the thin film surface remained almost the same as that of the substrate modulation [see Fig. 5(b)].

Spectrophotometric measurements recorded reflection maps for the fabricated sample. Linearly polarized light was used for two perpendicular polarizations: s and p , where s polarization is parallel to the grating lines on the sample. The angle between the normal of the grating and the detector was varied from 0° to 15° by steps of 0.5° . The resulting reflection maps are presented in Figs. 5(c) and 5(e).

The measured reflection maps of the sample correspond well to those following from the RCWA simulations. The

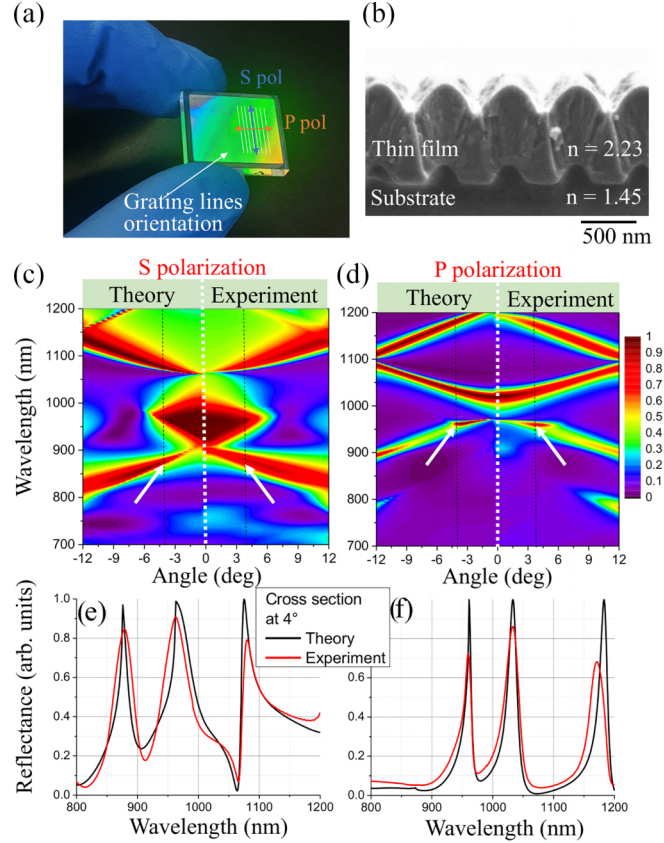


FIG. 5. Experimental results, compared with RCWA results: photo of fabricated samples (arrows indicate polarization directions) (a), and the SEM image of the specimen sample cross section (b). Numerical and experimental maps of the reflection in the plane of angle wavelength for (c),(d) s polarization and (e),(f) p polarization, with their cross sections at 4° of light incidence angle. The arrows indicate the points where the left and guided modes cross the continuum boundary.

lines of the Fano resonances were observed, narrowing and terminating at the EOC, and indicating the sharply peaked shapes; see Figs. 5(c)–5(f).

Remarkably, the sharply peaked resonances were indicated not only for the s polarization, as predicted by the above analysis, but also for p polarization. Also, both interfaces of the thin film were modulated. Current technical limitations of thin film fabrication did not allow us to obtain the modulation of only one interface, which strictly corresponds to the analytically studied cases. This indicates that the predicted and observed effect is generic (which is not restricted to the Schrödinger equation model), and robust with respect to nonessential modifications of the geometry of the driven potential.

VI. SUMMARY

We predicted a critical narrowing and the sharpening of the peak of the resonances when their eigenfrequencies approach the EOC. Importantly, the maximum reflection coefficient remains unity. We realized the effect for the wave propagation or reflection through the thin films with periodically modulated interfaces, and we demonstrated the predicted effect

measuring reflection coefficients depending on the frequency and incidence angle.

For the usual Fano resonances, the gain function g_0 is imaginary valued and symmetric, which gives a smooth variation of the phase delay of the response from 0 to π , with a value $\pi/2$ at the resonance, as well as a smooth peak of the resonance curve. In the reported case the gain function g_0 changes from imaginary to real at the EOC, which gives an abrupt $\pi/2$ jump of phase delay, as well as an unusual sharply peaked shape of the resonance.

To demonstrate the essence of the effect, we intended to isolate the points corresponding to the EOC, which allows us to interpret the phenomena in frames of a maximally simple model of only one guided wave. Additional effects could be expected at the coalescence of such two exceptional points corresponding to left- and right-guided waves. The crossing resonance lines in parameter space (θ, λ_0) , corresponding to left- and right-guided waves, can form in this plane sharply

edged triangles, which could be used for efficient spatial filtering. For instance, such spatial filtering effects were realized in [23,24] using the crossings of the usual, symmetric smooth-top resonance lines of Lorentzian form. Here, the asymmetries and sharp features of the coalescing resonances at the edge of the continuum can lead to advanced spatial filters with exotic characteristics, like sharp edges and flat tops, among others.

ACKNOWLEDGMENTS

This work has received funding from the Spanish Ministerio de Ciencia e Innovación under Grant No. 385 (PID2019-109175GB-C21), the European Social Fund (Project No. 09.3.3- LMT-K712-17- 0016) under a grant agreement with the Research Council of Lithuania (LMTLT), and also from the Horizon 2020 ERA.NET-COFUND program project MiLaCo (Project No. S-M-ERA.NET-20-2) under a grant agreement with the Research Council of Lithuania (LMTLT).

-
- [1] L. D. Landau and L. M. Lifshitz, *Quantum Mechanics: Non-relativistic Theory, 3rd ed., Course of Theoretical Physics* Vol. 3 (Butterworth-Heinemann, Amsterdam, 1981).
 - [2] Y. Wang, J. Song, L. Dong, and M. Lu, *J. Opt. Soc. Am. B* **33**, 2472 (2016).
 - [3] D. A. Bykov, E. A. Bezus, and L. L. Doskolovich, *Phys. Rev. A* **99**, 063805 (2019).
 - [4] S. S. Wang and R. Magnusson, *Appl. Opt.* **32**, 2606 (1993).
 - [5] Y. Ding and R. Magnusson, *Opt. Express* **12**, 5661 (2004).
 - [6] M. Shokooh-Saremi and R. Magnusson, *Opt. Express* **16**, 18249 (2008).
 - [7] R. Magnusson, *Opt. Lett.* **38**, 989 (2013).
 - [8] H. Kwon, D. Sounas, A. Cordaro, A. Polman, and A. Alù, *Phys. Rev. Lett.* **121**, 173004 (2018).
 - [9] A. Cordaro, H. Kwon, D. Sounas, A. F. Koenderink, A. Alù, and A. Polman, *Nano Lett.* **19**, 8418 (2019).
 - [10] H. Kwon, A. Cordaro, D. Sounas, A. Polman, and A. Alù, *ACS Photonics* **7**, 1799 (2020).
 - [11] D. Rosenblatt *et al.*, *IEEE Quantum Electron.* **33**, 2038 (1997).
 - [12] I. Evenor, E. Grinvald, F. Lenz, and S. Levit, *Eur. Phys. J. D* **66**, 231 (2012).
 - [13] L. Grineviciute, J. Nikitina, C. Babayigit, and K. Staliunas, *Appl. Phys. Lett.* **118**, 131114 (2021).
 - [14] F. Brückner *et al.*, *Opt. Lett.* **36**, 436 (2011).
 - [15] A. Bunkowski *et al.*, *Classical Quantum Gravity* **23**, 7297 (2006).
 - [16] See Supplemental Material at <http://link.aps.org/supplemental/10.1103/PhysRevA.107.L061501> for the two-dimensional (2D) RCWA app solver, which is used for numerically simulated results in Figs. 1–5.
 - [17] U. Fano, *Nuovo Cimento* **12**, 154 (1935).
 - [18] M. G. Moharam *et al.*, *J. Opt. Soc. Am. A* **12**, 1068 (1995).
 - [19] M. G. Moharam *et al.*, *J. Opt. Soc. Am. A* **12**, 1077 (1995).
 - [20] K. Reichelt and X. Jiang, *Thin Solid Films* **191**, 91 (1990).
 - [21] C. Bundesmanna and H. Neumann, *J. Appl. Phys.* **124**, 231102 (2018).
 - [22] L. Grineviciute, Nanostructured optical coatings for the manipulation of laser radiation, Doctoral thesis, Vilnius University, 2021.
 - [23] V. Purlys, L. Maigyte, D. Gailevičius, M. Peckus, M. Malinauskas, and K. Staliunas, *Phys. Rev. A* **87**, 033805 (2013).
 - [24] L. Grineviciute, C. Babayigit, D. Gailevičius, M. Peckus, M. Turdnev, T. Tolenis, M. Vengris, H. Kurt, and K. Staliunas, *Adv. Opt. Mater.* **9**, 2001730 (2021).